International Journal of Chemical Engineering– IJCE
Volume 2: Issue 1 [ISSN 2475-2711]
Publication Date: 30 October, 2015

Dry reforming of methane over Ni-La/SBA-15 based catalysts

[Rawaz Abdulrahman Ahmed[1*], Binta Abubakar Adama[2] and Samuel Shomefun[2]]

***Abstract*— Methane and carbon dioxide are the major components of biogas produced by anaerobic digestion of biomass and conversion of biogas to syngas is of great interesting for making use of the sustainable biomass resource. The present paper deals with catalyst development and testing for the dry reforming of methane (DRM). Three different lanthanum modified Ni catalysts were prepared using sequential impregnation, with nickel loadings from 9 to 16 wt. %, and lanthanum loadings from 5 to 23 wt. % based on support SBA-15. The catalysts were characterized by SEM/EDS, XRD, TPR and BET measurement. The mesoporous structure of the SBA-15 support was maintained and good dispersion of nickel and lanthanum nano-particles on the support were obtained for all prepared catalysts. The temperature programmed reduction (TPR) kinetics for these catalysts were analysed and the activation energies of the reaction was determined by using Kissinger method of analysis.**

The sample B was tested against the DRM, at different temperatures and catalyst weights, in order to assess their activity and selectivity. High methane conversion was achieved (100 %) at optimal condition. The mechanism of the reaction was assumed based on literature studies and rate equation was fitted to our experimental data. It was concluded that reforming temperature had an effect on the reaction mechanism.

***Keywords*— Ni-La-on-silica catalysts, TPR kinetics, DRM catalytic activity.**

I. Introduction

The dry reforming of methane has been of interest in recent years as it makes use of methane and carbon dioxide which are greenhouse gases and constitute to global warming [1]. The reaction produces synthetic gas with low H_2/CO (≤ 1) ratio which is a suitable feed for the Fischer-Tropsch synthesis of higher hydrocarbons [2]. The reaction looks straight forward but is accompanied by the side reactions including the reverse water gas shift reaction (RWGS), methane decomposition and the Boudouard reactions.

$CH_4+CO_2 \rightarrow 2H_2+2CO$ (dry reforming reaction)
$CO_2+H_2 \rightarrow H_2O+CO$ (RWGS)
$CH_4 \rightarrow C + H_2$ (methane decomposition)
$2CO \rightarrow C + CO_2$ (Boudouard Reaction)

Nickel catalysts are mostly used for DRM due to its availability and low cost [3] but the catalyst is easily deactivated by carbon deposition on the active sites due to methane decomposition and the Boudouard reaction. Therefore there is a need to develop and optimise nickel particles on the support in order to increase the stability and activity [2, 3] and this can be done by using different types of supports or using a promoter such as alkali and alkali earth metals. It is reported that the activity and performance of base catalysts were improved by this way [2]. Lanthanum oxides have been reported to help resist carbon deposition and help disperse nickel [4l. The literature reported that the reforming of methane with carbon dioxide over Ni/La_2O_3 catalyst was impressed due to present of La_2O_3 support. This is because of Ni particles were partially covered by $La_2O_2CO_3$ species which are formed by interaction of La_2O_3 with CO_2 [4]. Furthermore, Bradford and Vannice reported that the reforming of methane with carbon dioxide over Ni/MgO catalyst was both active and very stable [5]. This is because of the formation of a partially reducible NiO—MgO solid solution, which appears to stabilize the reduced nickel surfaces and provide resistance to carbon deposition [5].

This work presents the preparation of lanthanum modified nickel catalysts supported on mesoporous SBA-15 silica and the use of them for DRM reaction. A modified sol-gel method was chosen for the support preparation and impregnation method was used to incorporate the active phase, namely nickel, onto the support. The efficiency of prepared Ni-La/SBA-15 catalysts for DRM reaction was studied with regard to catalyst composition and reaction conditions and optimal catalyst and operating conditions were obtained.

II. Experimental

A. *Materials*

Tri-block copolymer Poly(ethylene oxide)-block-poly(propylene oxide)-block-poly(ethylene oxide) ($EO_{20}PO_{70}EO_{20}$, P_{123}, typical M_n = 5800), tetraethyleorthosilicae (TEOS), and DL-lactic acid 90% in water were purchased from Sigma-Aldrich and hydrochloric acid 37%, nickel nitrate hexahydrate 99%, nickel acetate and ammonium hydroxide 35% were from Fisher Scientific, UK. All chemicals were used as received. Deinoised water was used throughout the experiments.

B. *Catalyst synthesis*

Three Ni-La/SBA-15 catalysts were synthesized by a sol-gel method, with different Ni and La loading. The processing condition and the final composition of the resulting supported catalysts are also listed in Table 1.

R. Ahmed [1]

1-Kurdistan Institution for Strategic Studies and Scientific Research (KISSR) / Qirga, Slemani, Al Sulaymaniyah, Iraq
[*]Corresponding author
R. Ahmed[1], B. Adama[2] and S. Shomefun[2]
2 –School of Science & Engineering, Teesside University , Middlesbrough, Tees Valley, TS1 3BA, United Kingdom

Table 1. The preparation conditions of catalysts.

Ni-nitrate	La-nitrate	catalysts	Ni/La % loading
1.52	0.67	9IMPNi5LaN-A	9/5
2.00	1.33	13IMPNi23LaN-B	13/23
2.50	2.00	16IMPNi12LaN-C	16/12

IMP = impregnation; N = nitrate.

C. *Characterisation*

BET specific surface area and pore size distribution were determined by N_2 adsorption using a Belsorp-mini of BEL JAPAN Inc at 77 K after degassing the samples at 200°C for 3 hours. The BJH (Barret-Joyner-Halenda) method was used to calculated pore size distribution and pore volume. XRD data were obtained on a Bruker D8 diffractometer (Cu Kα, λ=0.1543 nm, $20^\circ < 2\Theta < 80^\circ$) [6]. SEM micrographs were obtained on a Hitachi S-3400N, Scanning Electron Microscope equipped with energy dispersive spectroscopy (EDS). TEM observations were done with a JEM2010F TEM, with a resolution of 0.23 nm, and accelerating voltage 80 to 200kV.

0.021g of the catalyst samples were reduced using 5%H_2/Ar mixture in a HIDEN ANALYTICAL CATLAB reactor using different heating rates (5°C/min, 10 °C /min, 15°C/min and 20 °C/min) from room temperature to 550 °C. It was kept at that temperature for 2hrs. The flow rate of the gas used was 20ml/min. The reduction peaks were obtained and analysed using the Kissinger equation [7]

$$\ln\frac{\beta}{T_{max}^2}=\ln\frac{AR}{E_a}-\frac{E_a}{RT_{max}} \quad (1)$$

Where β = heating rate, T-max and α-max are the absolute temperature and the degree of conversion at the maximum mass-loss rate $(d\alpha/dt)_{max}$, respectively. A is the pre exponential factor and Ea is the activation energy.

Catalysis of DRM was tested using catalyst 13NiIMP23LaN-B. Different weights of the catalyst were reduced using hydrogen of flow 20ml/min from room temperature to 550°C using a heating rate of 15°C/min and was kept at that temperature for 1 hour. The reforming reaction was carried out under integral steady state conditions in a CATLAB reactor using different catalyst weights of 0.015g, 0.025g and 0.035g at different reaction temperatures of 550°C, 600°C and 650°C. A ratio of 1.5:1.0 of CH_4:CO_2 was used. CO_2 and CH_4 flow rate of 40ml/min and 60ml/min, respectively were used. The conversions and yields were calculated as follows:

$$\%CH4=\frac{CH_4\text{in-}CH_4\text{out}}{CH_4\text{in}}\times100\% \quad (2)$$

$$\%CO_2=\frac{CO_2\text{in-}CO_2\text{out}}{CO_2\text{in}}\times100\% \quad (3)$$

$$YH_2=\frac{H_2\text{out}}{2CO_2\text{in}}\times100\% \quad (4)$$

$$YCO=\frac{CO\text{out}}{CO\text{out}+CO_2\text{ out}+CH_4\text{out}}\times100\% \quad (5)$$

Where Y is the yield.

$$H_2/CO\text{ ratio} = YH_2/YCO \quad (6)$$

III. Results and discussion

Figure 1 shows the low angle XRD pattern of the silica support for accommodating the nickel nanoparticles. Peaks denoted as (d_{100}), (d_{110}) and (d_{200}) are associated with a hexagonal symmetry (p6mm) [8], revealing that the mesoporous are arranged over long range order.

Figure 2A presents the TEM images of the SBA-15 sample, aged for 24 hr. The mesopores are arranged in a hexagonal honeycomb-like structure, separated by thin amorphous silica pore walls (black). The pores are reasonably straight with the pore size of approximately 7.6 nm in diameter and the pore wall thickness about 3 nm. The most striking fact about the SBA-15 material is that, although composed of amorphous silica, it displays a highly ordered structure with uniform mesopores which are big enough to accommodate catalytic components and are accessible for a range of molecules. This makes it very suitable to be a catalyst support.

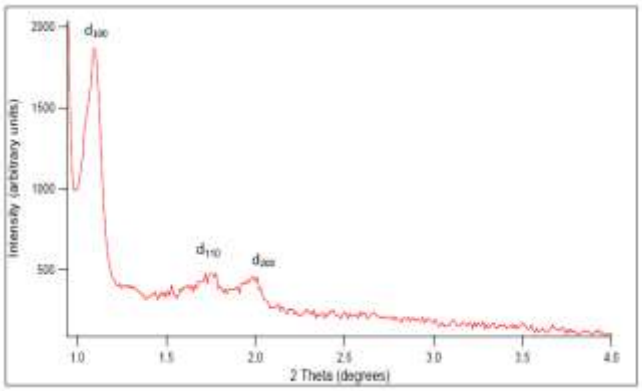

Figure 1. Typical low angle XRD pattern of SBA-15 synthesized in this study.

Figure 2B and C demonstrate the typical N_2 adsorption-desorption curves and the pore size distribution of the SBA-15 sample used in this research. It follows the type IV isotherm and H1 hysteresis loop, according to IUPAC classification. Clear adsorption step of capillary condensation at intermediate relative pressure was observed, indicating quite large mesoporous diameter and uniformity of the framework mesoporosity. This confirms that the SBA-15 has monomodal narrow pore size distribution, centred at around 3 (desorption) and 3.8 nm (adsorption), and the pore diameter is 7.6 nm, as it

was expected using BJH method [9,10]. The calculated BET-specific surface area is 834 m^2/g for this sample.

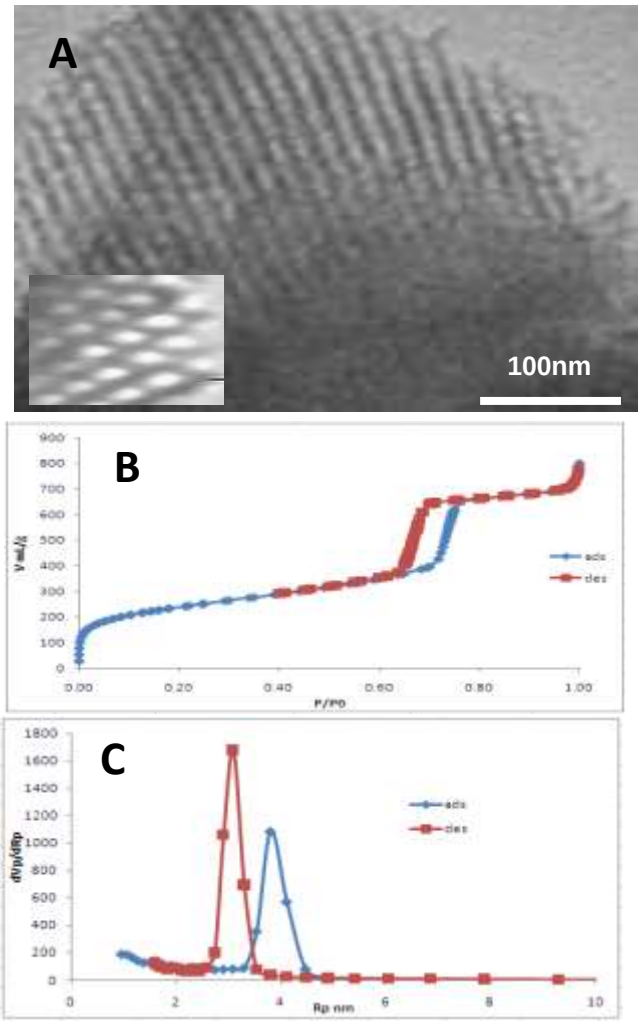

Figure 2. A) TEM micrograph, B) N_2 adsorption/desorption & C) pore size distribution of SBA-15 support.

The EDX results were taken from different areas of each sample; they show only little difference in the Ni loadings, proving that a good dispersion was achieved even at higher Ni loadings. The nickel species have migrated from the channels to the external surface and small crystallites of nickel oxide can be observed for samples with higher NiO/SiO_2 ratios (see Figs. 3A, 3B and 3C).

A high NiO/La_2O_3 ratio indicates a high dispersion of nickel oxide particles. The great value of the NiO/La_2O_3 ratio for the Ni catalysts (see Table 1) reflects that small NiO particles are located on the external surface or inside the mesochannel of SBA-15 silica, even for sample B. Particularly, 13IMPNi23LaN-B catalyst (see Fig. 3B) has the highest dispersion of NiO on the support. This catalyst has the highest La_2O_3 loading as obtained in the EDX analysis. This confirms that the promoter helps in the dispersion of NiO on the support. This is also evidenced through the wide-angle XRD results (see Fig. 5) and can be explained by the strong interaction of mixed Ni precursors with La metal on the SBA-15 support. Probably the higher dispersion of sample B comes from higher La_2O_3 loading (23 wt. %) comes from quite high Ni loading (13 wt. %). It is worthy of notice that the level of nickel dispersion is well correlated with the strength of nickel-lanthanum on support interaction.

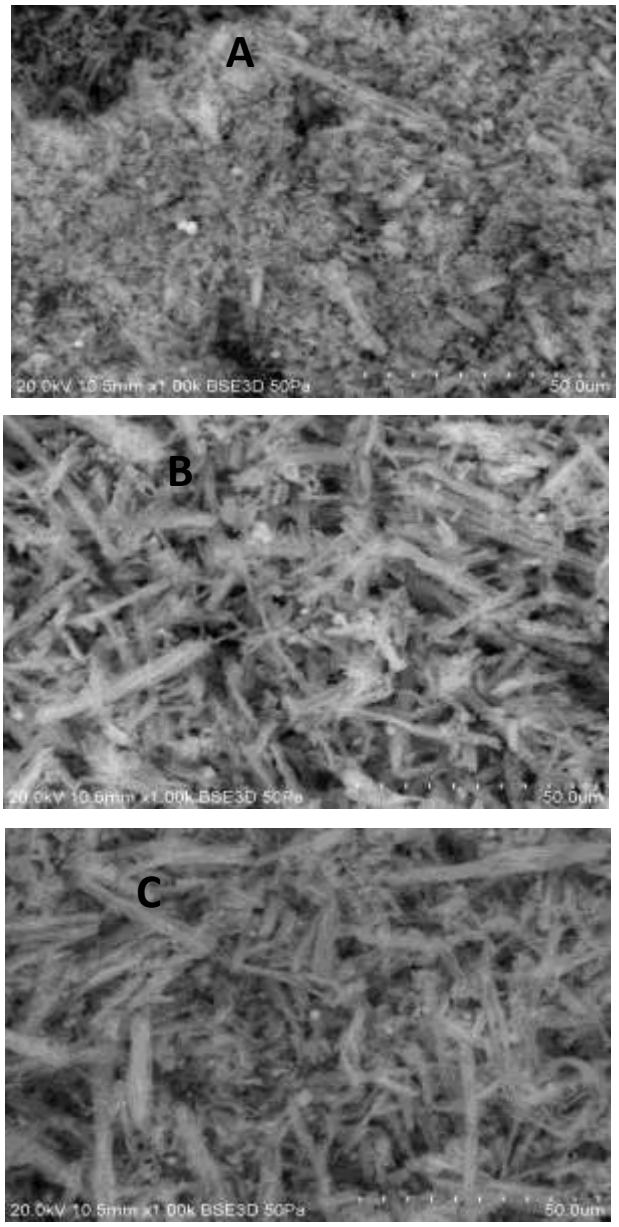

Figure 3. SEM image of A) 9IMPNi5LaN-A, B) 13IMPNi23LaN-B and C) 16IMPNi12LaN-C catalysts.

In addition to EDX, the SEM morphologies of all samples are shown in Fig. 3A, B and C. The influence of the Ni loading on the catalysts' morphology can be assessed by comparing samples A, B, and C. As observed, the morphologies are very similar to each other. Grey evidences the presence of nickel oxide, while white evidences the presence of silica. At low Ni loading (Fig. 3A) SEM shows homogeneous particles, with a fine distribution structure. It can be concluded that for

impregnation with low concentration solutions homogeneous morphologies are obtained. At higher Ni loading (Fig. 3B), the morphology appears to be as a large fibrous structure of 30–80 μm in length and 10–20 μm in diameter are clearly evidence in comparison with other sample the size of the modified material by increasing the La metal, can significantly change on the morphology of Ni based catalyst. In the SEM image for catalyst C the morphology appears to be as a fibres similar to the structure of sample B , with very fine organized impact structure. It seems that the long fibre-like structure has been disconnected, due to effect of high Ni loading.

According to the low-angle XRD results, shown in Fig. 4, the mesoporous structure of the support is maintained after nickel impregnation. Before and after impregnation, the silica and nickel-containing silica should all possess similar mesoporous structures, as reported [8]. All the three samples display at least three reflections: (100), (110) and (200), characteristic for hexagonal array of mesochannels [8] and confirming the impregnation has no noticeable influence on the mesostructured of support. In Fig. 5, the wide-angle spectra showed strong NiO peaks for 9IMPNi5LaN-A and 16IMPNi12LaN-C catalysts indicating large NiO clusters presence in the catalysts, whilst very weak peaks were observed for the 13IMPNi23LaN-B catalyst, indicating a high dispersion of NiO on the support. This also shows the effect of La_2O_3 promoter on the catalyst – helps dispersion of the NiO on the SBA-15 support, as 13IMPNi23LaN-B catalyst has highest La_2O_3 among the three catalysts.

Table 2: kinetic parameters of the two reduction peaks

Sample	Ea_1 (kJ/mol)	A_1	Ea_2 (kJ/mol)	A_2
9IMPNi5LaN-A	63.79	44707	101.70	8.37E+08
13IMPNi23LaN-B	25.15	10669	60.49	1.52E+08
16IMPNi12LaN-C	56.96	15733	80.46	30376

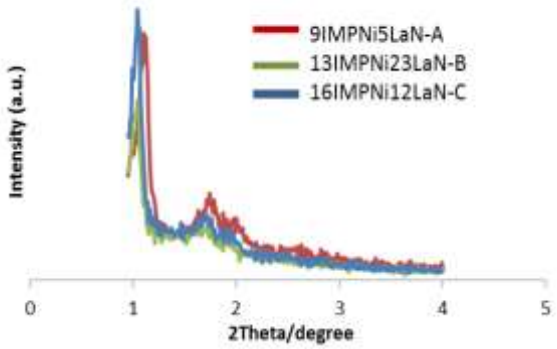

Figure 4. Low-angle XRD of catalysts.

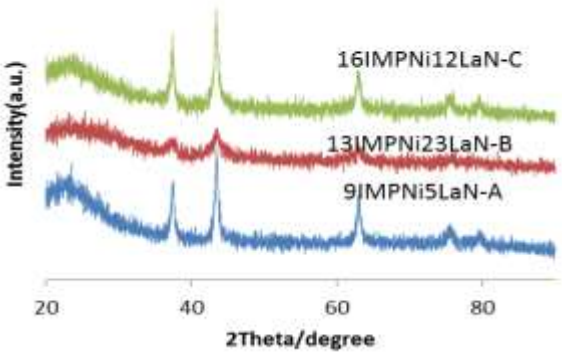

Figure 5. Wide-angle XRD of catalysts.

The TPR profiles of the samples at 10 ^oC heating rate are shown in Fig. 6. For the 9% of Ni sample A, reduction peaks are at 350 ^oC and 514 ^oC , respectively. Similarly, the 16% of Ni sample C has reduction peaks at 340 ^oC and 520 ^oC. However, the reduction peaks for 13% of Ni sample B are at 187 ^oC and 370 ^oC. The lower temperature peaks of the samples is attributed to the reduction of weakly interacted NiO on the silica support. The higher the interaction the higher the reduction temperature [11]. The temperature at first reduction peak of the 13% of Ni sample B is the lowest which shows the effect of La_2O_3 as reported by Li et al [12].

It also means that NiO on the silica support is more homogenous and has a higher dispersion, which makes the active component easier to reduce [12]. The broadness of the first reduction peak for the 13% of Ni sample B show high Ni interaction with the silica support [13]. Each reduction peak for the samples was analysed and the activation energies were determined using equation 1 and are tabulated in Table 2 where Ea_1 and Ea_2 are the activation energies of the first and second reduction peak , respectively.

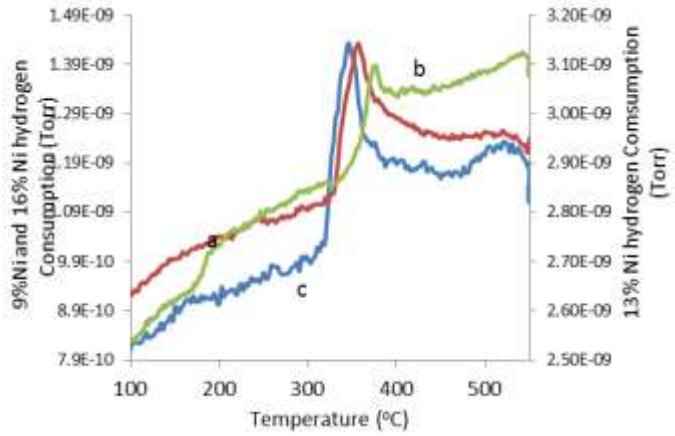

Figure 6 TPR profile of a) 9IMPNi5LaN-A, b) 13IMPNi23LaN-B and c) 16IMPNi12LaN-C catalysts at 10 ^{o}C heating rate .

The 13IMPNi23LaN-B catalyst is optimal as it has the highest reducibility and the lowest reduction activation energy and thus was chosen for DRM tests. Figure 7 shows the conversion of CO_2 as a function of the reaction temperature where it is observed that the conversion increases with increasing catalyst weight as expected. This is because the contact time (W/Fa_o) which depends on the catalyst weight and the inlet gas flow rate increases with increasing weight as the inlet flow rate of the gases were kept constant. The H_2/CO ratio were calculated and the ratio was always above unity which implies that hydrogen is not used by the RWGS reaction different from the study done by Pan et al [11] where the reforming reaction study was done over Ni/SiO_2 catalyst. This suggests that the presence of the La_2O_3 modifier helps suppress side reactions. Table 3 shows that CH_4 conversion is always lower than that of CO_2 as the latter is the limiting reactant. The high activity of the catalyst may be attributed to the absence of strong alkaline promoter as La_2O_3 is only slightly basic [14]. Strong basic promoters help to hinder the accumulation of coke but also results in a significant reduction of catalyst activity [14].

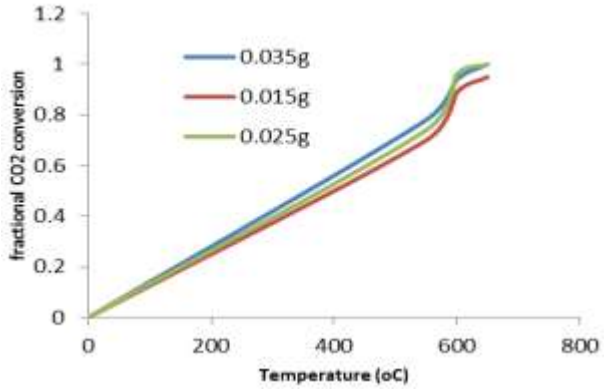

Figure 7 Change of conversion with temperature and catalyst weight of 13IMPNi23LaN-B sample.

There are some studies done on the kinetics of dry reforming on Ni/La_2O_3 proposing the reaction mechanism. Verykios [5] proposed that CH_4 dissociates to deposit carbon on the catalyst and liberate hydrogen. CO_2 reacts with La_2O_3 to form oxy-carbonate ($La_2O_2CO_3$). The oxy-carbonate then reacts with the carbon deposited on the site to form CO and La_2O_3. The RDS was assumed to be the methane dissociation and the surface reaction steps. This mechanism was also proposed by Moradi et al [3].

$$CH_4 + s \overset{K1}{\leftrightarrow} s\text{-}CH_4 \ (\text{equilibrium})$$

$$s\text{-}CH_4 \overset{k2}{\rightarrow} s\text{-}C + 2H_2 \ (\text{RDS})$$

$$CO_2 + La_2O_3 \overset{K3}{\leftrightarrow} La_2O_2CO_3 \ (\text{equilibrium})$$

$$La_2O_2CO_3 + C\text{-}s \overset{k4}{\rightarrow} La_2O_3 + 2CO + s \ (\text{RDS})$$

Assuming that the H_2 and CO coverage on the support is negligible the reaction rate is:

$$r_{CO_2} = \frac{K_1 k_2 K_3 k_4 P_{CH_4} P_{CO_2}}{K_1 k_2 K3 P_{CH_4} P_{CO_2} + K_1 k_2 P_{CH_4} + K_3 k_4 P_{CO_2}} \quad (7)$$

Where K_1 is the equilibrium constant for the methane adsorption, k_2 is the rate constant for the methane decomposition reaction, K_3 is the equilibrium constant for the reaction of CO_2 and La_2O_3 and k_4 is the rate constant for the oxy-carbonate reaction. The values of the constants are given in Table 4 in terms of temperature as obtained by Verykios [5]. Graphs of the conversion against the contact time were plotted in Fig. 8 showing an increase in conversion with increase in the space time as previously discussed.

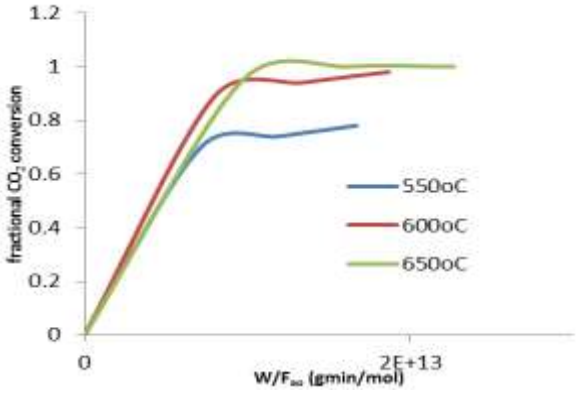

Figure 8 Change of conversion with contact time for 13IMPNi23LaN-B sample.

$$\frac{W}{Fao} = \int_0^x \frac{dx}{r_{CO_2}} \quad (8)$$

The above equation (8) was integrated at different CO_2 conversions to find the contact time using equation 8 obtained from literature [5].

Table 3: CO_2 and CH_4 Conversion against weight change.

Conversion %	0.015g	0.025g	0.035g
	CO_2 % Conversion		
550°C	70	74	78
600°C	89	94	96
650°C	95	100	100
	CH_4 % Conversion		
550°C	57	60	63
600°C	61	78	78
650°C	85	86	86

Table 4: Kinetic parameters .

Parameters	NiO/ La_2O_3
K_1k_2 (mol/g s (kpa)$^{-1}$	2.61 x 10^{-3} exp(-4300/T)
K_3 (kpa)$^{-1}$	5.17 x 10^{-5} exp(8700/T)
k_4 (mol/g s)	.35 x 10^{-1} exp(-7500/T)

The rate data obtained from literature as shown in equation 7 was fitted with our experimental data and graphs of the fitness were produced. It was observed that the calculated data closely fit the observed experimental conversion for the reaction temperature of 600°C as shown in Fig. 9. The data however, did not fit our experimental data at reaction temperatures of 550°C and 650°C.
The RDS of the reforming reaction changes with reforming temperature as reported in literature. Cui et al [1] concluded that in temperature ranges of 550 – 575°C the dissociation of methane becomes the RDS. In the temperature range of 650 – 750°C the surface reaction of adsorbed species becomes the rate determining step. At temperature ranges of 575-650°C there are two RDSs as seen from our result.

From the analyses, a catalyst was chosen and studied for the CO_2 reforming of CH_4. In order to develop a catalyst with a high performance, it is necessary to determine the reaction mechanism and the rate determining steps (RDS). Many authors have reported different kinds of mechanism and RDSs for the reforming reaction. Bradford and Vannice [4] proposed that there are 2 RDSs: the CH_4 dissociation step and the CH_xO decomposition. Verykios [5] also proposed that the RDSs for the reforming reaction over Ni/La_2O_3 catalyst involve methane decomposition and the reaction of carbon species on the catalyst surface and $La_2O_2CO_3$ formed from the reaction with CO_2. Cui et al [1] reported that the reaction temperature affects the reforming mechanism and the RDSs at different temperature regions. In this paper, mechanisms obtained from literature were proposed for the reaction obtained from literature and fitted to our experimental data.

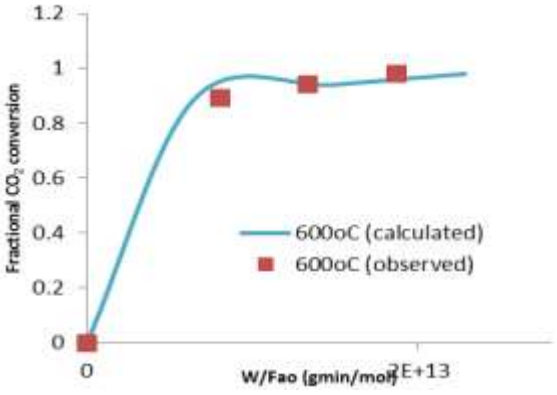

Figure 9: Fitness of kinetic data at 600°C.

IV. Conclusion

In this work, three Ni/La_2O_3 samples were prepared and characterized using various techniques. The 13IMPNi23LaN-B with highest La content has the best NiO dispersion onto the support among the three samples according to XRD results, confirming the effect of La_2O_3 promoter on the dispersion of NiO particles. Also the hexagonal structure of the support was maintained after impregnation of the two metals.

The TPR results showed two reduction peaks for all three samples and the lowest reduction temperature is obtained for the 13IMPNi23LaN-B sample. This shows that La_2O_3 increases the reducibility of the catalyst. This was also proven by the activation energy (Ea) of the reduction of the 13IMPNi23LaN-B being the lowest. The catalyst showed high activity which increased with increase in the weight of the catalyst used and the reaction temperature. The RWGS reaction was suppressed as indicated by the H_2/CO ratio higher than unity. The CO_2 conversion data at 600°C well fits the kinetics of reaction mechanism from literature [3,5,14] , but the data at 550°C and 650°C do not, because the mechanism and/or RDS of the reaction is different at these temperatures from 600°C.

References

1. Cui, yuehua, et al. "*Kinetic Study of the catalytic reforming of CH_4 with CO_2 to syngas over Ni/Al_2O_3 calalyst: the effect of temperature on the reforming mechanism".*, Applied Catalysis A: General, (2007) , pp. 79-88.
2. Barroso-Quirogs; M., M. and Casteo-Luna; A. E. *"Catalytic Activity and effect of modifiers on Ni-based catalysts for the dry reforming of methane*", International Journal of hydrogen energy, 35 (2010), pp. 6052-6056.
3. Sharifnia; S., Rahmanzadeh; M and Moradi; G.R ".*Kinetic Investigations of CO_2 reforming of CH_4 over La-Ni based perovskite", Chemical Engineering Journal, 162 (*2010).
4. Verykios; X. E. " *Catalytic dry reforming of natural gas for the production of chemicals and hydrogen"* , International Journal of Hydrogen Energy, 28(2003), pp. 1045 – 1063.
5. Bradford; M. C. J. and Vannice; A. M. "*Catalytic reforming of methane with carbon dioxide over nickel catalsysts", Applied catalysis A: General*, 142(1996), pp.73-96.
6. Hufschmidt, D., Bobadilla, L.F., Romero-Sarria, F., Centeno, M.A., Odriozola, J.A., Montes, M., Falabella, E. "Supported nickel catalysts with a controlled molecular architecture for the catalytic reformation of methane" , Catalysis Today, 149 (2010) 394-400.
7**.** Mentus; A. and Jankovic, B**. "***The kinetic Study of temperature -programmed reduction of nickel oxide in hydrogen atmosphere",* Chemical Engineering Science, 63(2008).
8. Strock, S., Bretinger, H. and Maier, W. F. "Characterization of micro and mesoporous solids by physisorption methods and pores size analysis", Applied Catalysts, 174(1998) 137-146.
9. Impe´ror-Clerc, Davidson, M., P., and Davidson, A.. "Existence of a Microporous Corona around the Mesopores of Silica-Based SBA-15 Materials Templated by Triblock Copolymers" , Journal of the American Chemical Society, 122 (2000) 11925-11933.
10. Anunziata, O. A., Martínez, M. L. and Beltramone, A. R.. "Hydroxyapatite/MCM-41 and SBA-15 Nano-Composites: Preparation, Characterization and Applications", Materials, 2 (2009) 1508-1519.
11. Pan; Y.-X., Liu; C.-J. and Shi; P. "*Preparation and Characterization of Coke resistant Ni/SiO_2 catalyst for carbon dioxide reforming of methane", Journal of Power Source , 176(2008),pp.43-56.*
12. Li, X. , Hu; Q., Yang; Y.,Chen; J. and Lai; Z. "*Effects of Sol gel method and lanthanum addition on catalytic performances of nickel-based catalysts for methane reforming with carbon dioxide*", Journal of Rare Earths , 26 (2008), p. 864-868.
13. Rivas; I., Alvarez; J., Pietri; E., Perez-Zurita; M. S., Godwasser; R. M. "*Perovskite-type oxides in methane dry reforming: Effect of their incorporation into a mesoporous SBA-15 silica-host",* Catalysis Today, 149(2010), pp.388-393.
14. Zhang; Z. and Verikios; X. E. "C*arbon dioxide reforming of methane to synthesis gas over Ni/La_2O_3 catalysts",* Applied Catalysis A: General, 138(1996), pp.109-133.